Low Turn-On Voltage and High Focus Capability for Field Emission Display

Yi-Ting Kuo, Hsiang-Yu Lo and Yiming Li

Department of Communication Engineering, National Chiao Tung University, Hsinchu, Taiwan

ABSTRACT

In this work, the properties of low turn-on voltage and high focused capability for novel field emission display are studied. According to the development of novel structure for surface conduction electron-emitter provided by Tsai et al, the 3D FTDT-PIC method has been used to analyze the properties of this device. We can find the novel structure having a tip around the corner on the left electrode implies that it can produce high electric fields around the emitter apex, and generate high emission current.

Keywords: low turn-on voltage, high focus capability, field emission display, nanogap, FDTD-PIC

1 INTRODUCTION

Nanometer scale gaps (nanogaps) has been wildly used as electrode in molecular electronics [1,2], biosensor [3], and vacuum microelectronics [4]. However, the difficulty from the fabrication limits the development of such technique until the surface conduction electron-emitter (SCE) for the flat panel displays (FPDs) has been provided by Sakai et al [5]. Recently, the field emission efficiency of the SCE device has been studied, and the result shows the structure of the nanogap similar to the type 1 in Fig. 1 will be helpful to generate the high field emission efficiency [6]. After Tsai et al [7] have succeeded in fabricating a new type of SCE device using hydrogen absorption under high pressure treatment. A well-defined gap size and simple process can be given by this method which is accompanied by extensive atomic migration during the hydrogen treatment.

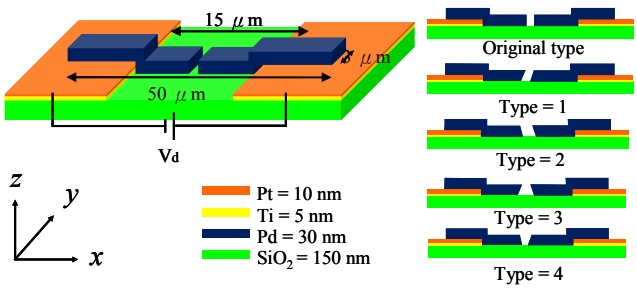

Figure 1: The schematic of the emitter structures and the five types of the nanogap due to the process variation.

To change the angle of the conventional nanogap results in the better emission efficiency using the type 1 in Fig. 1 [6]. The direction of the nanogap in type 1 provides a path for the electron trajectory with lower collision. The similar property is expected for the novel SCE device. In this paper, to explore the electron-emission behaviors in the novel SCE device, the FDTD-PIC simulation technique [6] is employed to solve a set of 3D Maxwell equations coupled with the Lorentz equation. Moreover, the property of the low turn-on voltage and high focus capability in the novel SCE device has been analyzed in this study.

2 SIMULATION TECHNIQUES

Figure 2 represents the procedure of FDTD-PIC. The procedure of PIC starts from a specified initial state, and the simulated electrostatic fields is applied as its evolution in time. Then a time-dependent differential form of Faraday's law, Ampere's law, and the relativistic Lorentz equation are shown as follows:

$$\begin{aligned} \frac{\partial \mathbf{B}}{\partial t} &= -\nabla \times \mathbf{E}, \\ \frac{\partial \mathbf{E}}{\partial t} &= -\frac{\mathbf{J}}{\varepsilon} + \frac{1}{\mu\varepsilon}\nabla \times \mathbf{B}, \\ \mathbf{F} &= q\left(\mathbf{E} + \mathbf{v} \times \mathbf{B}\right), \text{ and} \\ \frac{\partial \mathbf{x}}{\partial t} &= \mathbf{v}, \end{aligned} \tag{1}$$

subject to constraints provided by Gauss's law and the rule of divergence of **B**,

$$\nabla \cdot \mathbf{E} = \frac{\rho}{\varepsilon} \text{ and } \nabla \cdot \mathbf{B} = 0. \tag{2}$$

that **E** and **B** are the electric and magnetic fields, **x** is the position of charge particle, and **J** and ρ are the current density and charge density resulting from charge particles. The full set of Maxwell equations is simultaneously solved to obtain electromagnetic fields. Similarly, the Lorentz force equation is solved to obtain relativistic particle trajectories. In addition, the electromagnetic fields are advanced in time at each time step. The charged particles are moved according to the Lorentz equation using the fields advanced in each time step. The obtained charge density and current density are successively used as sources in the 3D Maxwell equations for advancing the electromagnetic fields. These steps are repeated for each

time step until the specified number of time steps is reached. The FDTD procedure can be seen in Fig. 2 and PIC procedure in Fig. 3. In the FE process, the electron emission is modeled by the Fowler-Nordheim (F-N) equation

$$J = \frac{AE^2}{\phi\, t^2} \exp\left(\frac{-Bv(y)\phi^{3/2}}{E}\right). \quad (3)$$

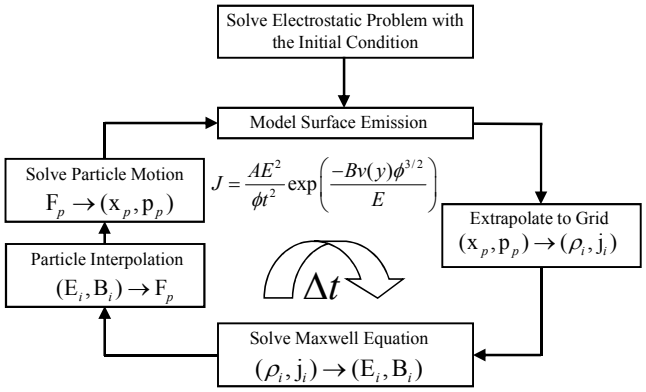

Figure 2: The computational scheme and the corresponding equations for the electron emission simulation.

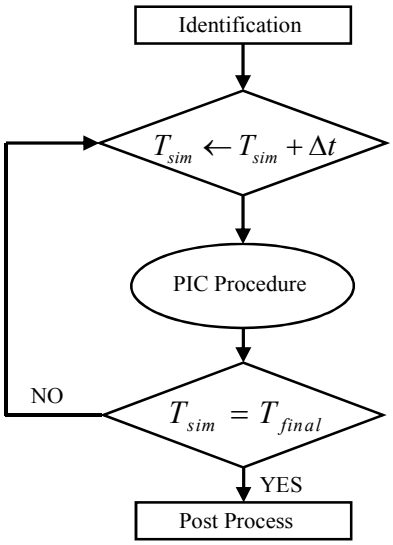

Figure 3: The computational scheme and the corresponding equations for the flowchart of PIC procedure.

3 COMPUTAIONAL RESULTS

The schematic of the novel emitter structures and related SEM images are shown in Fig. 4. The turn-on voltages for different spacing widths of both conventional and novel SCE devices are analyzed using the FDTD-PIC. The results show the novel structure produces the emission current 0.1 mA under lower turn-on voltage than the conventional one, which is represented in Fig. 5. This is because the tip of the novel structure generates the strong electric field intensity, especially for the narrower spacing of the nanogap, and such strong electric field in the vacuum improves the electrons tunneling from the Pd strip into vacuum. Hence for the same electric field intensity, the turn-on voltage for the structure with the tip is lower. Additionally, the turn-on voltage for both cases decreases due to the intensity of electric field becomes larger, which comes from the spacing width for the nanogap decreases. Hence the low turn-on voltage SCE devices can be achieved by reducing the spacing width for nanogaps. Table 1 shows the turn-on voltages for both structures under 30, 60, and 90 nm gap width. When the gap width is large, the turn-on voltage in the novel case is large due to the different heights for the two electrodes. Such electrodes make the electric field be small within the gap. However, as the gap width decreases, the turn-on voltage drops significantly in the novel case because the tip structure increases the electric field. Hence the turn-on voltage of the novel structure is smaller than the conventional one with the gap width smaller than 60 nm.

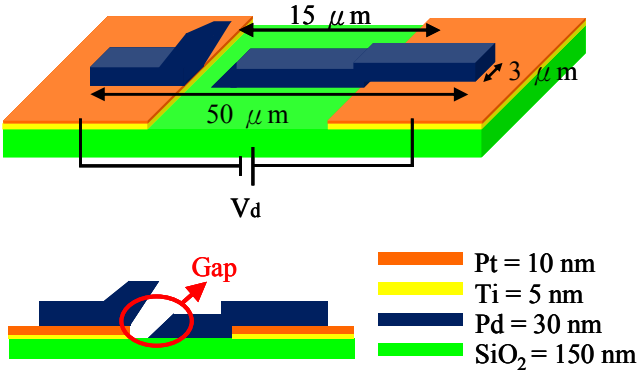

Figure 4: The schematic of the conventional (upper left) and novel emitter (upper right) structures and related SEM images (lower left one is conventional, and lower right one is novel).

Furthermore, the focus capability for both cases is simulated under the applied voltage is 60 V. The both conventional and novel SCE devices with 25 nm nanogaps are provided as examples. Figure 6 and 8 indicate the electron beam on both the x-z and y-z planes for the conventional SCE device. Figure 7 illustrates the electron trajectories near the nanogap on the x-z plane. The electron beam starts to spread on the y-z palne when electrons move far from the nanogap. It is due to the large fraction for the electrons and makes them collided with the driving electrode, such that electrons are scattered back into the vacuum. The simulated current density for the conventional SCE device is presented in Fig. 6. The current density spreads due to the scattered electrons.

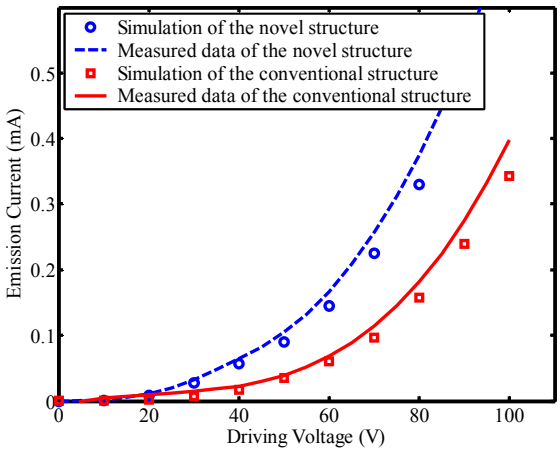

Figure 5: The I-V curves of the SCE devices with the 25 nm nanogap are given by conventional (in red) and novel (in blue) structures.

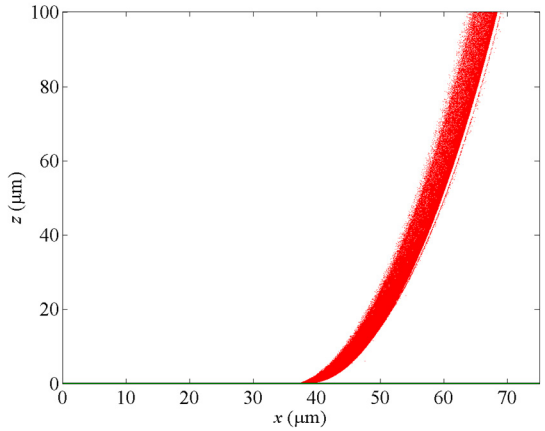

Figure 6: The electron beam on the x-z plane for the conventional SCE device with the 25 nm nanogap under applied voltage is 60 V

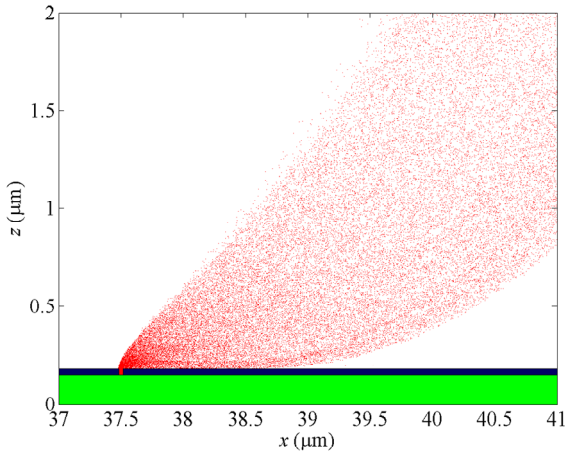

Figure 7: The zoom-in plot of the Fig. 6 near the nanogap.

Method \ Width	30 nm	60 nm	90 nm
Focus Ion Beam	60 V	85 V	160 V
Hydrogen Embrittlement	50 V	80 V	200 V

Table 1: The turn-on voltage for different structures under various gap widths.

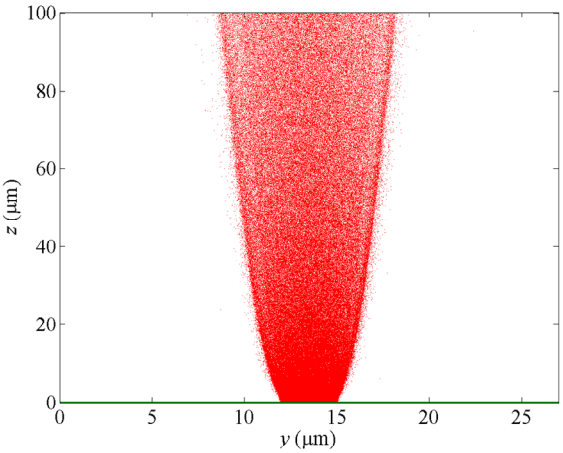

Figure 8: The electron beam on the y-z plane for the conventional SCE device with the 25 nm nanogap under applied voltage is 60 V.

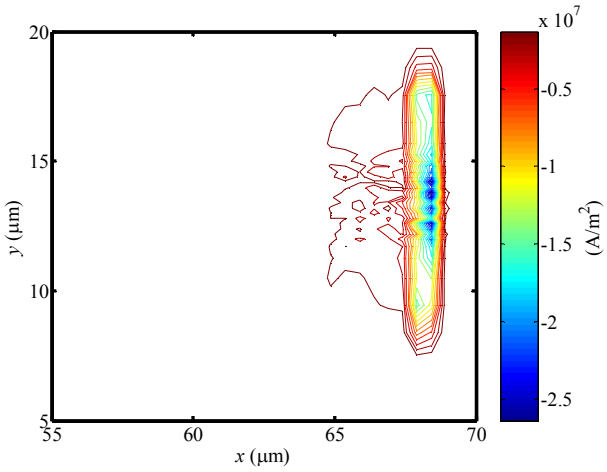

Figure 9: the simulated current density distributions on the anode plates for the conventional SCE structures with the 25 nm nanogap under applied voltage 60 V.

For the novel case, Figure 10 shows the electron trajectories on the x-z plane. The zoom-in plot, as shown in Fig. 11, illustrates the fewer collided particles with the opposite electrode comparing with the conventional case, as shown in Fig. 7. Furthermore, the new structure effectively

NSTI-Nanotech 2008, www.nsti.org, ISBN 978-1-4200-8505-1 Vol. 3

reduces the fraction between the electrons and the driving electrode, so that the electron beam does not spread, as shown in Fig. 12. As the result, the simulated current density shows the better focus capability for the novel SCE device.

4 CONCLUSIONS

We have applied the 3D FDTD-PIC simulator to analyze the new SCE device provided by Tsai et al [7] and to show the advantages of such new structure. The conventional and novel SCE devices with 25 nm nanogaps are provided to verify the simulation result with the experiment one. The simulation and experiment results agree well to each other. Consequently, the advantages of low turn-on voltage, high focus capability are convinced for the novel SCE device.

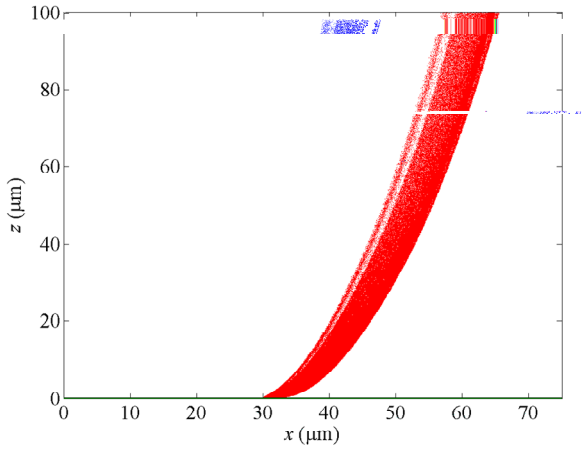

Figure 10: The electron beam on the x-z plane for the novel SCE device with the 25 nm nanogap under applied voltage is 60 V.

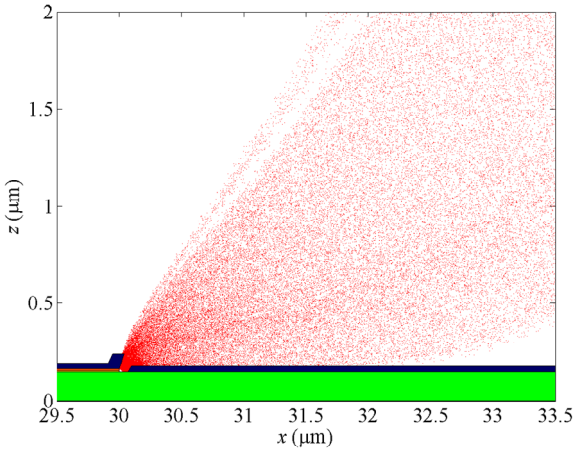

Figure 11: The zoom-in plot of the Fig. 10 near the nanogap.

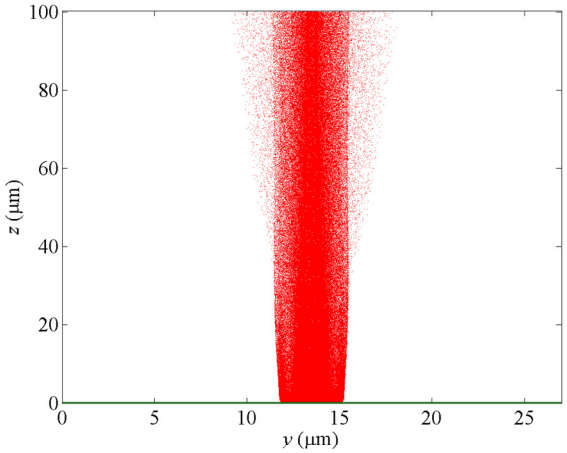

Figure 12: The electron beam on the y-z plane for the novel SCE device with the 25 nm nanogap under applied voltage is 60 V.

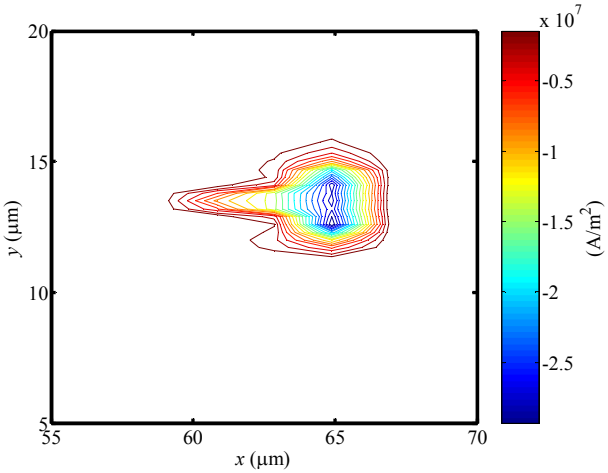

Figure 13: the simulated current density distributions on the anode plates for the novel SCE structures with the 25 nm nanogap under applied voltage 60 V.

REFERENCES

[1] Reed M A, Zhou C, Muller C J, Burgin T P and Tour J M, Science 278 252-4, 1997.

[2] Linag W, Shores M P, Bockrath M, Long J R and Park H, Nature 417 725-9, 2002.

[3] Yi M, Jeong K H and Lee L P, Biosens. Bioelectron. 20 1320-6, 2004.

[4] Lee H I, Park S S, Park D I, Ham S H and Lee J H 1, J. Vac. Sci. Technol. B 16 762-4, 1998.

[5] E. Yamaguchi, K. Sakai, I. Nomura., J. Soc. Inf. Disp. 5, 345, 1997.

[6] H.-Y Lo, Y Li, H.-Y Chao, C.-H Tsai, F.-M Pan, M.-C Chiang, M. Liu, T.-C Kuo, and C.-N Mo, Proc. IEEE Nano, 353, 2007.

[7] C.-H Tsai, F.-M Pan, K.-J Chen, C-Y, Wei, M. Liu, and C-N, Mo, Appl. Phys. Lett. 90 163115, 2007.